minerals

MDPI

Review

Stable Isotope Imprints during Pyrite Leaching: Implications for Acid Rock Drainage Characterization

Ágnes Ódri [1,*], Megan Becker [1,2], Jennifer Broadhurst [1], Susan T. L. Harrison [1,3] and Mansour Edraki [4]

1 Minerals to Metals Initiative (MtM), Department of Chemical Engineering, University of Cape Town, Private Bag X3, Rondebosch, Cape Town 7701, South Africa; megan.becker@uct.ac.za (M.B.); jennifer.broadhurst@uct.ac.za (J.B.); sue.harrison@uct.ac.za (S.T.L.H.)
2 Centre for Minerals Research, Department of Chemical Engineering, University of Cape Town, Private Bag X3, Rondebosch, Cape Town 7701, South Africa
3 Centre for Bioprocess Engineering Research, Department of Chemical Engineering, University of Cape Town, Private Bag X3, Rondebosch, Cape Town 7701, South Africa
4 Centre for Mined Land Rehabilitation, Sustainable Minerals Institute, The University of Queensland, St Lucia, Brisbane, QLD 4072, Australia; m.edraki@cmlr.uq.edu.au
* Correspondence: odriagnes@gmail.com

Received: 1 September 2020; Accepted: 1 November 2020; Published: 4 November 2020

Abstract: The characterization of acid rock drainage (ARD) is traditionally based on mineralogical and geochemical techniques (e.g., Acid Base Accounting tests). The complexity of ARD processes warrants contribution of methods from various disciplines. In the past decade, the increasing role of environmental isotopes in pollution monitoring has enabled the successful application of isotope methods in ARD investigations. While isotopic compositions of different pollutants can refer to their parent mineral, the degree of isotope fractionations are indicative of the mechanisms taking place during the release and transportation of ARD-related contaminants. In natural environments, however, the measured isotope fractionations are predominantly the result of several coexisting or sequential processes. Therefore, the identification and quantification of the distinct contributions of these processes to isotope variations is difficult and requires well-defined laboratory conditions, where the influence of ARD generation on different isotope systems can be assessed with greater certainty. This review provides readers with a single source of information regarding isotopic variations generated by laboratory pyrite leaching.

Keywords: stable isotopes; acid rock drainage; pyrite leaching; mine waste; tailings

1. Introduction

Acid rock drainage (ARD) is one of the major environmental problems at active and closed coal and metalliferous mining sites [1]. ARD forms naturally when sulfidic material comes in contact with atmospheric oxygen and the oxidation of sulfide minerals releases acid and contaminants. Although, pyrite is the most common sulfide in nature and is widely regarded as the main cause of ARD, other sulfides including arsenopyrite and iron-rich sphalerite also contribute to ARD generation [2–4]. The process is slow in nature, but the increase of contact surface areas at mine sites due to the excavation of mine workings and production of waste accelerates the rate of acidic drainage generation [5]. The large-scale ARD that is generated within the mining area is called acid mine drainage (AMD). Oxidative dissolution of sulfide minerals not only acidifies the environment, but also allows soluble metals and salts to enter into the solution phase and to be transported outside the mining site boundaries by surface and groundwater systems [6–8]. Metal pollution associated with acidic effluents has toxic effects on aquatic ecosystems,

wildlife, surrounding vegetation and soil ecosystem [9–11]. Also, ARD affected soils are physically degraded and characterized by high concentrations of deleterious elements [12]. The high acidity increases the availability of soluble metals that affects the microbial activity, microbial community structure, biomass, and nutrient production [13,14]. Because of the potential remobilization of accumulated metals, these acidic soils can be considered as secondary sources of pollution.

The water levels in the mine workings are kept to a minimum during active mining. However, after mine closure, rising and particularly fluctuating water levels increase the risk of ARD generation [15]. For example, water that refills the underground workings due to the ceased pumping dissolves the mineral precipitates from sulfide oxidation that have accumulated on the pore space of the exposed walls and ceilings of the workings during the operation. These secondary minerals tend to store metals, metalloids, acidity, and sulfate [16,17], and their dissolution results in an initial drainage with higher acidity and metal contents (called first flush phenomena) than the subsequent ARD. On the surface, the exposure of residual sulfide minerals to water and air in waste storage facilities leads to ARD formation. The small particle sizes of mine tailings (<0.2 mm) [18] has the potential to enhance the rate of oxidation owing to increased sulfide liberation.

To characterize and predict ARD accurately, the fundamental controls on ARD generation including pH, temperature, redox conditions, type and concentration of oxidants, mineralogy, and textural characteristics need to be understood. These factors influence the oxidation and dissolution rate of pyrite. For example, the increase of the concentration of oxidants (Fe^{3+} and O_2), temperature, and Eh of solution result in accelerated pyrite dissolution rates under acidic conditions [19]. At the same time, the source and various attenuation reactions of pollutants both at the early stage of ARD formation and during their subsequent solute transport need to be identified. Formation of secondary water-soluble iron phases and minerals not only affects the ARD chemistry but also influences pyrite oxidation dynamics directly and indirectly by providing H^+ and/or Fe^{3+} and changing the mineralogy of the oxidized layers of pyrite [20,21]. The latter has significance in surface passivation that, in turn, affects the reaction rates of pyrite oxidation and dissolution. Several field and laboratory tests have been developed to characterize ARD generation potential and inform modelling studies for ARD prediction [22,23]. Static tests generate Acid Base Accounting (ABA) and Net Acid Generation (NAG) data and give an indication of the acid generating and neutralizing potential of mine wastes. These methods are considered static in nature as they do not provide information about the rate of acid production or neutralization [24–26]. Laboratory kinetic tests (e.g., humidity cells test) provide insight into ARD generation rates [27,28]. More detailed column leach tests have been developed in recent years for modelling, but due to their complex and time-consuming nature, their application remains limited [29]. Detailed mineralogy of mine waste is also suggested to inform ARD characterization [30–32] and reduce uncertainty or error in static and kinetic tests [33]. In addition, the compositional heterogeneity of pyrite can result in resistivity variations that affect its chemical reactivity and leaching behavior [34–37]. The oxidation potential of pyrite with various trace element composition is also relevant for accurate ARD characterization. Whereas the traditional ARD characterization tests involve mainly geochemical and basic mineralogical approaches, the analytical techniques for accurate measurement of a wide range of environmental isotopes have undergone continual refinement over the past few decades and present a powerful analytical approach in pollution monitoring [38,39]. In addition to the source identification by comparing isotopic composition of contaminants and their potential sources, the redistribution of stable isotopes between different phases during physicochemical and biotic processes help to understand the mechanisms that trigger the isotopic variations [40,41]. The isotope technique has the potential to complement the classic ARD characterization tests effectively because static and kinetic tests do not provide information about the source of various ARD contaminants and their fate during transportation. To apply different isotope systems as indicators of physicochemical or biotic processes, it is essential to know the degree of isotopic fractionation to relate it to different mechanisms. In nature, the isotopic variations are controlled by several coexisting or sequential processes that are difficult to distinguish based on the "sum total" of the different fractionation factors. This review, therefore,

provides an overview on the application of sulfur, oxygen, and iron isotope analyses in the interpretation of different reaction mechanisms taking place during the oxidative dissolution of pyrite under controlled laboratory conditions. The aim is to highlight potential research areas where this information can be applied and where the isotope technique is not routinely used yet. A summary of the fundamentals of stable isotope geochemistry and ARD generation is provided in Section 2. In Sections 3 and 4, the behavior of sulfur and oxygen isotopes during the oxidative dissolution of pyrite is presented, followed by that of the iron isotopes in Section 5. Finally, the summary and future perspectives are presented.

2. Stable Isotopes in ARD-Related Processes

The different isotopes of a given element have distinct number of neutrons, and thus different masses. Mass differences cause variations in their physical characteristic and reactivity that ultimately results in the partitioning of heavier and lighter isotopes during physicochemical and biological processes [42]. The degree of partitioning of different isotopes between two co-existing reservoirs is mainly controlled by mass-dependent kinetic and equilibrium laws [43,44] and described by the isotopic fractionation factor:

$$\alpha_{A-B} = \frac{R_A}{R_B} \quad (1)$$

where R is the ratio of the heavy isotope to the light isotope, and A and B denote the two co-existing phases, chemical compounds, or the isotope ratio of a starting material and the product. As the value of α is very close to 1, the degree of fractionation can also be approximated by the difference in isotopic composition of two reservoirs, if delta values are <10 per mil (‰) [45]:

$$1000 \ln \alpha_{A-B} \approx \delta_A - \delta_B \approx \Delta_{A-B} \quad (2)$$

where δ notation reports the per mil differences in the isotopic ratios of a sample relative to an internationally accepted standard:

$$\delta x\ (‰) = \frac{R_{sample} - R_{standard}}{R_{standard}} \times 1000 \quad (3)$$

x refers to the type of the isotope, and R is the ratio of the heavy isotope to the light isotope in the sample (R_{sample}) and in the reference ($R_{standard}$).

The oxidation of sulfide minerals takes place through several chemical reactions, as shown here for pyrite in Reactions (4)–(6) [46]:

$$FeS_2 + 3.5O_2 + H_2O \rightarrow Fe^{2+} + 2SO_4^{2-} + 2H^+ \quad (4)$$

$$Fe^{2+} + H^+ + 0.25O_2 \rightarrow Fe^{3+} + 0.5H_2O \quad (5)$$

$$FeS_2 + 14Fe^{3+} + 8H_2O \rightarrow 15Fe^{2+} + 2SO_4^{2-} + 16H^+ \quad (6)$$

The rate of Reaction (6) is limited by the oxidation of Fe^{2+} in Reaction (5), which is greatly catalyzed by iron oxidizing microbial species such as *Acidithiobacillus ferrooxidans* by up to five orders of magnitude [47]. Other key microbial species involved include *Leptospirillum ferriphilum*, *Acidiplasma cupricumulans,* and *Ferroplasma* species [48,49]. Therefore, the rate of pyrite oxidation via Fe^{3+} can be enhanced by several orders of magnitude compared to the abiotic oxidation via O_2 (from 18 to 170 times more rapid than the Reaction (4)) [47,50].

Reactions (4)–(6) demonstrate only the overall stoichiometry of pyrite oxidation that is generally recognized as a complex, multistep chemical, electrochemical, and bacterially mediated mechanism [51]. Numerous studies have suggested that pyrite oxidation/dissolution rates in aqueous solutions are controlled by electrochemical processes that depend on the semiconducting properties of pyrite [52–58]. This type of dissolution involves the distinct anodic and cathodic sites on the pyrite surface where

electron transfer reactions occur during the oxidation and reduction processes. The oxidation of pyrite under the moist-air settings typical of mine waste piles is considered both chemical and electrochemical [35,59]. The contribution of these two mechanisms to pyrite oxidation is still highly debated as well as the intermediate steps of ARD formation [60,61]. As stable isotopes are intensively involved in these reactions, they may provide a potential tool to identify the different intermediate mechanisms that control the ARD generation [52,61–65].

3. Sulfur Isotope Signatures of Pyrite Leaching

Sulfur isotope composition of dissolved sulfates in ARD relates to the source of sulfur, therefore it has the potential to be successfully used in mass balance calculations as part of the pollution monitoring [66–69].

Pyrite leaching experiments demonstrate that the quantitative conversion of pyrite to sulfate results in only minor sulfur isotope fractionation ($\Delta^{34}S_{SO4–FeS2}$) under acidic, aerobic-biotic, or abiotic conditions ranging between −1.3‰ and +0.4‰ [63,70–74]. In addition, processes like precipitation and dissolution of secondary sulfate phases were demonstrated to produce negligible S isotope fractionation (e.g., $\Delta^{34}S_{schwertmannite–sulfate}$ −0.2‰ – +0.3‰ and $\Delta^{34}S_{H\text{-}jarosite–sulfate}$ +0.3‰ – +1.1‰) [75–77]. Although these relatively small S isotope fractionation factors allow the identification of the parent sulfides in ARD-impacted water, the seasonal precipitation and dissolution cycles of sulfate minerals might cause small variations in the isotopic composition of sulfate as well. Bioleaching of pyrite at pH 2.05 by Brunner et al. [78] showed a fractionation factor of −0.2‰, in agreement with previously determined fractionation values [63,70–74]. In addition, inconsistent isotopic signatures of SO_4 were demonstrated throughout the pyrite dissolution, where the initial phase of the experiment was characterized by high $\delta^{34}S$ values compared to parent mineral and only moderate $\delta^{34}S$ enrichment was determined in the main stage (Figure 1) [78]. The weaker correlation and lower slope of the initial phase of the experiment suggests that processes other than sulfur leaching from pyrite affect the sulfur isotope composition of sulfates. The authors of Brunner et al. [78] concluded that the degassing of SO_2 at the beginning of the experiment enriches the residual aqueous SO_4 in the heavier sulfur isotope (^{34}S) due to the dominant kinetic isotope effect of this conversion. The loss of SO_2 is also in accordance with the non-stoichiometric initial pyrite dissolution findings described by others, where the molar ratio of SO_4^{2-}/Fe^t was 1.1 for biotic leaching and ranged from 1.5 to 1.6 for abiotic leaching at pH 1.2 to 2 [79,80]. Sulfur isotope fractionation values of +0.4‰ and −1.3‰ were obtained by Pisapia et al. [73] during the non-stoichiometric and stoichiometric phases of their biotic, aerobic (<pH 2) pyrite dissolution experiments. The authors of Pisapia et al. [73] attributed the opposing positive and negative $\Delta^{34}S_{SO4–FeS2}$ values to different pyrite oxidation pathways and did not relate the ^{34}S enrichment of sulfate directly to SO_2 degassing.

According to the overall stoichiometry of pyrite oxidation mechanisms, abiotic oxidation can take place only when there is enough dissolved oxygen to complete the reaction [81]. This suggests that although Reactions (4) and (6) are the most frequently used pathways to demonstrate pyrite oxidation, the actual mechanisms are much more complex and involve the occurrence of intermediate sulfur species like thiosulfate ($S_2O_3^{2-}$), elemental sulfur (S^o), and sulfite (SO_3^{2-}), depending on the availability of oxygen. The authors of Basolo and Pearson [82] argue that, according to the overall oxidation reactions of pyrite, seven electrons are transferred from the mineral to the oxidant, but because it is unlikely that more than two electrons are transferred at a time, pyrite oxidation always requires intermediate steps to produce sulfate (Figure 2). The formation of sulfur intermediates during abiotic and biotic pyrite oxidation was confirmed by several authors both under acidic and alkaline conditions, reporting systematically smaller amounts of intermediates at lower pH due to their rapid oxidation to sulfate [52,53,60,80,83–89]. The mechanism of microbial oxidation of sulfide minerals at low pH occurs via thiosulfate or polysulfide pathways [90]. The different dissolution reactions are a result of (i) differences between the crystal structures of acid-soluble and non-acid-soluble metal sulfides and (ii) the distinct oxidizing strategies used by different microorganisms [91]. Pyrite–as an acid-insoluble sulfide–is mostly oxidized by bacterially generated Fe^{3+} through the thiosulfate pathway by breaking

the Fe–S bonds of the mineral. The Fe^{3+} ion is reduced to Fe^{2+} after accepting an electron from pyrite and becomes re-oxidized by microbes. The reduction-oxidation cycles continue until Fe^{2+} and thiosulfate are released from the pyrite, resulting ultimately in sulfate as the end-product via the oxidation of thiosulfate → tetrathionate → sulfite oxyanions (Figure 2). With respect to circumneutral and alkaline pH values, tetrathionate and sulfate formation takes place at pH 6–7, whereas thiosulfate and sulfite are formed at pH 9 [84]. In the polysulfide pathway, acid-soluble sulfides, e.g., sphalerite (ZnS) and chalcopyrite ($CuFeS_2$), are dissolved by both Fe^{3+} and H^+, allowing protons to break M-S bonds in the sulfides [90,92]. The main sulfur intermediates from these reactions are polysulfides (S_n^{2-}) and elemental sulfur, which may eventually oxidize to sulfate (Figure 2). Nevertheless, polysulfide formation has been detected alongside sulfate and minor iron-oxides from acidic pyrite oxidation by *A. ferrooxidans* under experimental aerobic conditions [73].

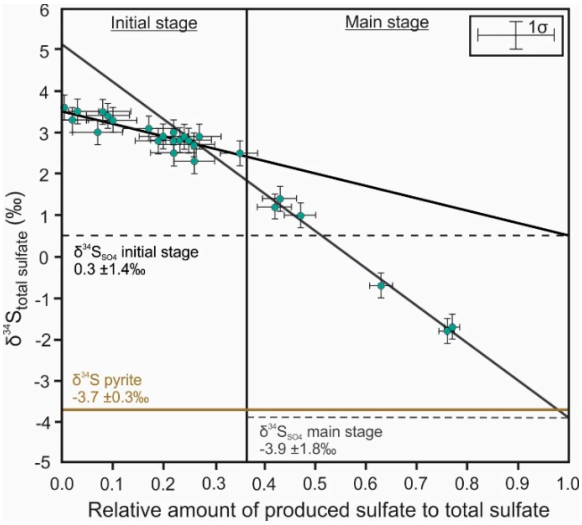

Figure 1. $\delta^{34}S$ variations of sulfates as a function of their increasing amount during the initial and main stages of pyrite leaching. The dashed lines show the $\delta^{34}S$ values of sulfate that are produced in the initial and the main stages. The vertical line demonstrates the transition from the initial to the main stage of pyrite leaching. Redrawn from Brunner et al. [78].

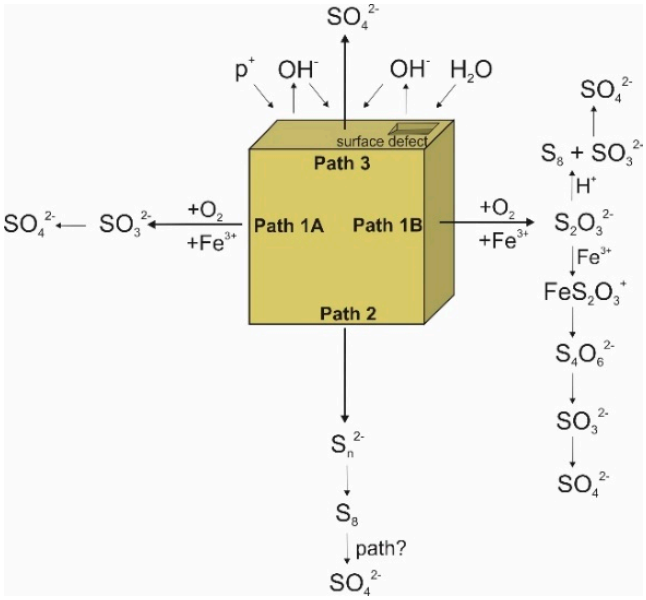

Figure 2. Schematic representation of different sulfide oxidation pathways: Paths 1A and 1B represent thiosulfate oxidation pathways where thiosulfate detaches and where the S–S bond breaks instead of

the Fe–S bond releasing sulfite directly [90]. Path 2 represents the sulfide–polysulfide-elemental sulfur pathway of monosulfides [90] and Path 3 represents the defect/photochemically driven pathway where surface electron defects can initiate pyrite oxidation by surface water and drive the subsequent sulfur oxidation by OH^- [93]. Figure modified from Druschel and Borda [94].

The incomplete oxidation of pyrite or its stepwise oxidation to sulfate is frequently accompanied by sulfur isotope variation in agreement with the general concepts of isotope fractionation, and the more oxidized form of sulfur is enriched in the heavier isotope compared to more reduced forms [52,95,96]. The redistribution of sulfur isotopes in association with the oxidation of different sulfur compounds was demonstrated by experimental and field studies under various conditions [53,72,74,97–101]. As S and O isotopes of sulfate are intensively involved in redox reactions that control the sulfur oxyanion formations, the isotope fractionation has the potential to provide insight on the governing pathways of sulfur oxidation or reduction. Due to the complexity of these redox processes along with the large number of variables that control the sulfur conversion mechanisms (e.g., residence time of sulfur intermediates, pH, crystal structure of the leached mineral, bacterial occurrence, oxygen availability, dominant oxidant), current understanding of the influence of sulfur intermediates on both the ARD sulfur cycle dynamics and its isotope geochemical characteristics is relatively limited.

4. Oxygen Isotope Signatures of Pyrite Leaching

The oxygen isotope composition of dissolved sulfate can be used to understand the oxidation reaction pathways of sulfide minerals. Sulfate-generated via pyrite oxidation-preserves its oxygen isotope composition after formation both due to the very slow kinetics of oxygen isotope equilibration between water and sulfate [102–104] and the small fractionation between dissolved sulfate and secondary sulfate minerals during precipitation (average $\Delta^{18}O_{precipitate–sulfate}$ +0.5‰ – +0.6‰) [76]. This allows for the identification of the reaction mechanisms that are responsible for sulfide oxidation. If most of the sulfate oxygen is derived from the dissolved molecular oxygen via Reaction (4), the emerging SO_4 should be enriched in ^{18}O relative to SO_4 that incorporates dominantly water-derived oxygen (WDO) following Reaction (6). The reason for this is that air is characterized by $\delta^{18}O$ = +23.8 ‰ [105–107], whereas meteoric water has variable $\delta^{18}O$ values, mainly $\delta^{18}O \leq 0$ ‰ [108]. Using Equations (7) and (8), the relative contributions of WDO and molecular oxygen to dissolved sulfate can be calculated [64].

$$\delta^{18}O_{SO4} = X(\delta^{18}O_{H2O} + \varepsilon_{H2O}) + (1 - X)\,(\delta^{18}O_{O2} + \varepsilon_{O2}) \quad (7)$$

where X is the fraction of sulfate produced by Reaction (6) and (1 − X) is the fraction of sulfate from Reaction (4). ε is the enrichment factor that describes the partition of oxygen between the sulfate and air or water. $\varepsilon^{18}O_{SO4\text{-}H2O}$ = 0.0‰ to +4.1‰ for both anaerobic biotic and abiotic experiments and $\varepsilon^{18}O_{SO4\text{-}O2}$ = −10.0‰ to −11.4‰ for biotic and −4.3‰ to −9.8‰ for abiotic reactions [63,64,72]. By measuring the $\delta^{18}O_{SO4}$ and $\delta^{18}O_{H2O}$, Equation (7) can be re-arranged according to Equation (8) [99]:

$$\delta^{18}O_{SO4} = X(\delta^{18}O_{H2O} + \varepsilon_{H2O} - \delta^{18}O_{O2} - \varepsilon_{O2}) + (\,\delta^{18}O_{O2} + \varepsilon_{O2}) \quad (8)$$

The above calculations require the assumption of both constant oxygen isotope enrichment factors and the lack of isotope exchange reactions between the water and dissolved sulfate after the oxidation.

The general concept regarding the relative percent contribution of various oxygen sources to sulfate is that: (i) if pyrite oxidation is anaerobic and Reaction (6) is the dominant, then 100% of the sulfate oxygen is derived from water, and (ii) if dissolved molecular oxygen is present, sulfate oxygen shows a combination of air and water oxygen [68,109–111]. The incorporation of WDO in sulfate is controlled by Fe oxidizing bacteria [112]. The overall pyrite oxidation reaction (Reaction (4)) suggests that 87.5% of sulfate oxygen is dissolved molecular oxygen and the remaining 12.5% is water derived. The $\delta^{18}O$ and

therefore WDO values of sulfate, however, do not necessarily reflect the stoichiometry of Reaction (4). Pyrite oxidation experiments conducted by Taylor et al. [63] showed that under water-saturated, anaerobic-abiotic and -biotic conditions at pH 2, mainly water oxygen is involved in the formation of sulfate, with WDO values of 94% and 65%, respectively. Their estimated WDO of sulfate during the alternation of wet and dry cycles in the absence of bacteria was 72%, whereas biotic wet and dry pyrite oxidation indicated the lowest value of 23%. These results demonstrate that pyrite oxidation is primarily controlled by Fe^{3+}, and biological reactions appear to incorporate more atmospheric oxygen in sulfate compared with abiotic mechanisms. The authors of Balci et al. [72], however, did not find a distinct microbial control on the pyrite oxidation pathways during the biotic and abiotic leaching experiments that were conducted under anaerobic, aerobic, and acidic pH conditions. According to their results, Fe^{3+} was the main oxidant for pyrite, and consequently, water oxygen was predominantly incorporated in sulfate. The short- and long-term experiments resulted in WDO values of 85% and 92% respectively, under aerobic-biotic conditions, and 87% for aerobic-abiotic reactions. Because of the similar estimated WDO values, Balci et al. [72] considered the incubation time and pH as the main controls on the oxygen isotope composition of sulfates. This is also in accordance with the results of Qureshi [113] which suggest pH as the major factor controlling the isotopic composition of sulfate.

To understand the reason for significant water oxygen incorporation into sulfate at low pH even under oxygen-saturated conditions, it is necessary to review the mechanism of pyrite oxidation. The initial step is the oxidation of the adsorbed $Fe^{2+}(H_2O)_6$ complexes on the pyrite surface by molecular oxygen to form $Fe^{3+}(H_2O)_6$ complexes that rapidly oxidize the pyrite (Figure 3) [53,87]. During the initial release of Fe^{2+} to solution, the pyrite surface is dominated by sulfur atoms [114]. The adsorbed iron continuously experiences oxidation and reduction during the interaction with molecular oxygen and the acceptance of electrons from the pyrite (Figure 3). The latter process is governed by the electron loss of iron on the pyrite surface during the interaction via molecular oxygen [52]. The electron originates from the sulfur site and its transmission to Fe^{3+} takes place via the iron site of the mineral (Figure 3b).

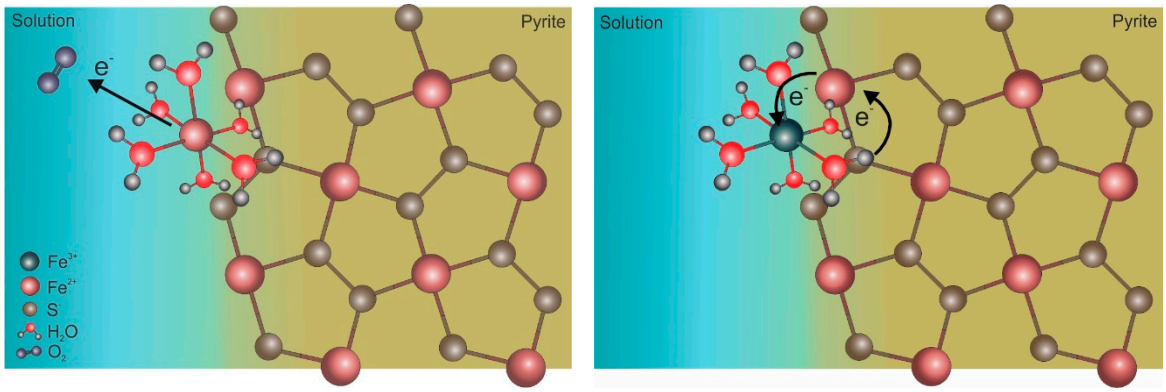

Figure 3. Illustration of the abiotic oxidation mechanism of pyrite. The adsorption of released Fe^{2+} from pyrite as aqueous $Fe^{2+}(H_2O)_6$ is the first step of pyrite oxidation. (**a**) The oxidation of $Fe^{2+}(H_2O)_6$ complex by the dissolved molecular oxygen forms (**b**) Fe^{3+} that accepts electron from the pyrite during its oxidation.

An oxygen atom from the adsorbed $Fe^{3+}(H_2O)_6$ complex is added to the sulfur site of pyrite as the closing step of pyrite oxidation that produces different sulfur intermediates (Figure 4a) [85,88,94]. The reaction sequence of the oxidation-reduction of the Fe^{3+} in the adsorbed aqueous complex, and the transfer of oxygen from water molecules to the sulfur site of pyrite, continues until a sulfur oxyanion is more stable in solution, and disassociates from the pyrite surface (Figure 4b) [53].

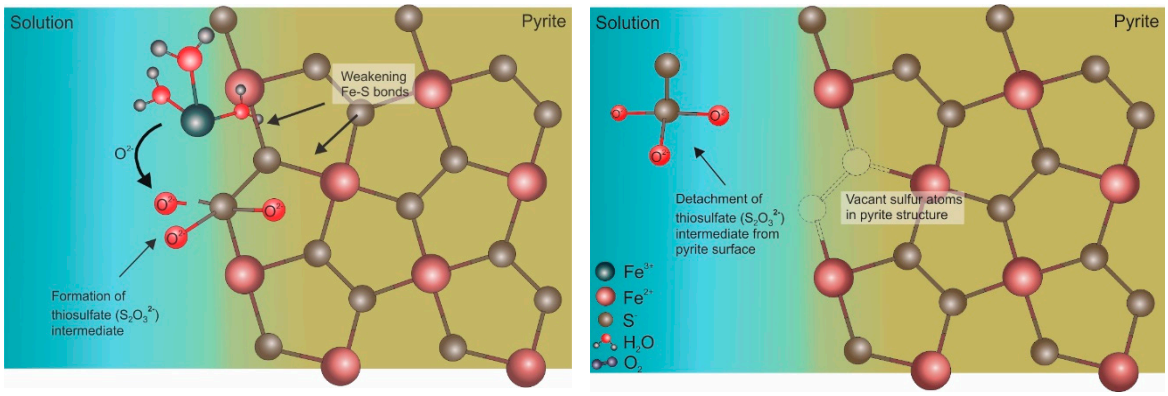

Figure 4. Illustration of the formation of sulfur oxyanion during the abiotic oxidation of pyrite using the example of thiosulfate. (**a**) Addition of oxygen molecules from the aqueous $Fe^{3+}(H_2O)_6$ complex to pyrite sulfur to form thiosulfate. (**b**) The oxygen transfer continues until the detachment of the stable thiosulfate.

In accordance with the mechanism described above, oxygen plays a role in the initiation of the pyrite oxidation reaction, but the reaction pathway is mainly controlled by Fe^{3+} as the oxidant. As molecular oxygen is not directly involved in the formation of sulfur oxyanion intermediates, the incorporation of water oxygen into thiosulfate from $Fe^{3+}(H_2O)_6$ complexes is the major process that affects the oxygen isotope composition of this sulfur compound [115]. Although these oxidation steps are consistent with the high proportion of WDO in the experimentally produced sulfates, these do not explain the minor contribution of atmospheric oxygen in the sulfur oxidation reactions. The dominance of water oxygen in the formation of sulfur intermediates suggests that the participation of molecular oxygen in sulfate takes place at the more advanced stages of oxidation. Figure 5 demonstrates that the transition of sulfite to sulfate is the only conversion during the oxidation sequence when O_2 may participate in the reactions. Consequently, if anything slows down or inhibits this oxidation step (e.g., a decrease in pH reduces the amounts of sulfur intermediates) [84] that would increase the relative contribution of WDO to sulfate.

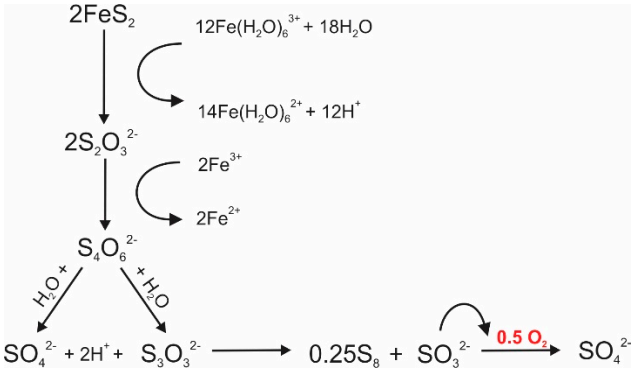

Figure 5. Pyrite oxidation pathway under oxygen-saturated conditions. Molecular oxygen–indicated in red–shows the incorporation of O_2 into sulfates. This oxidation step is considered to decrease the relative percent contribution of WDO to produced sulfate. Figure modified from Balci et al. [72].

The distribution mechanism of oxygen between water and sulfate based on their isotopic signatures was demonstrated by Brunner et al. [78]. Although the generated sulfate and water showed identical $\delta^{18}O$ value of 1.3‰ at the end of the pyrite dissolution, inconsistent oxygen isotope partitioning is presented on Figure 6. Sulfates are characterized by strong and various heavy oxygen isotope (^{18}O) enrichment at the initial stage, whereas these become isotopically lighter as a function of their

increasing amount during the main stage. At the start of dissolution, sulfates show ~2.0‰ lower $\delta^{18}O$ values relative to sulfate oxygen that would be derived from water characterized by $\delta^{18}O$ = 1.3‰. According to the authors of Brunner et al. [78], sulfite intermediates formed at the early stages of dissolution are not converted to sulfate immediately. This allows a prolonged initial oxygen isotope equilibration between sulfite and water that can lower the $\delta^{18}O$ values of the initial sulfates produced.

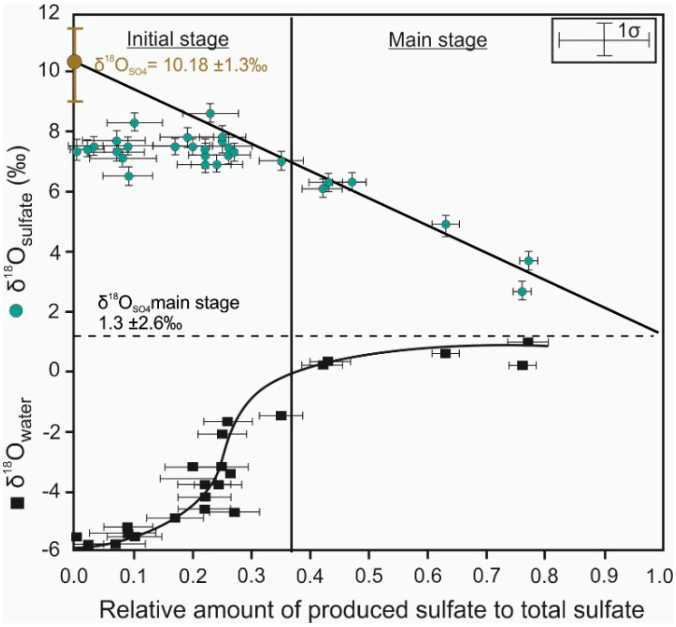

Figure 6. $\delta^{18}O$ variations of sulfates and interacting water as a function of the increasing amount of sulfate during pyrite leaching. The dashed line shows the $\delta^{18}O$ values of sulfate that are produced in the main stage of dissolution. The gold circle illustrates the supposed $\delta^{18}O$ value of initial sulfates in case of immediate conversion of sulfite to sulfate. The vertical line demonstrates the transition from the initial to the main stage of pyrite leaching. Redrawn from Brunner et al. [78].

Based on the above, the major potential factors that are considered to cause variations in sulfate oxygen isotope values and the ratio of WDO and O_2 are: (i) the contribution of different oxygen sources, (ii) degree of the oxygen isotope exchange between water and various sulfur intermediates, (iii) environmental conditions such as pH or availability of oxygen, and (iv) the reaction mechanisms of pyrite oxidation through the related sulfur intermediates [65,86,116].

5. Iron Isotope Signatures of Pyrite Leaching

The release of iron and other transition metals from sulfide minerals during oxidative dissolution can be demonstrated by the isotopic composition of both minerals and the solution [41,117]. Iron isotope variations were previously considered as biological signatures, however, Zhu et al. [118] demonstrated using the example of Cu and Fe that abiotic processes can also be responsible for the isotope fractionation of the transition metals. Fractionation of Fe isotopes have been recognized since the mid-1990s [119–121]. There is an overall agreement that changes in chemical conditions such as pH or redox potential strongly affect the mobilization of iron [122,123], but the interpretation of related Fe isotope variations is still under debate because of the relative novelty of the technique.

Laboratory experiments have shown that the dissolution reactions take place on the surface of the minerals and have demonstrated the dominance of kinetically controlled faster reaction rates of light isotopes (kinetic isotope effect) at the beginning of dissolution [124]. Wiederhold [125] found that during the reductive, abiotic leaching of goethite, the lighter Fe isotopes (^{54}Fe) were released into the solution at the early stages, which resulted in the enrichment of the heavier isotopes (^{56}Fe) at the mineral surface. However, the increase of the $\delta^{56}Fe$ value of the solution during the second stage

suggested both the dominance of the equilibrium isotope effect—the forward and backward reaction rates of isotopes are identical between product and reactant—and the transient role of the initial kinetic fractionation. The preservation of the initial isotope composition depends on the extent of dissolution. The kinetic fractionation can be overwritten and erased by the subsequent isotope effects in the case of completed dissolution, which would result in the identical isotopic signature of the solution and the reacting mineral.

Similar to reductive weathering, both kinetic and equilibrium isotope fractionation between coexisting Fe(II) and Fe(III) complexes in solution was also suggested by experimental studies under oxidative conditions [126,127]. Fractionation values of 2.63 ± 0.11‰ and 2.75 ± 0.01‰ were estimated between aqueous Fe(II) and precipitated Fe(III) at pH values of 5.5 and 2.5, respectively [128]. The authors of Anbar et al. [129] suggested a slightly higher fractionation of 3.0 ‰ between aqueous Fe(II) and Fe(III) complexes. The degree of Fe isotope fractionation during Fe(III) oxides and hydroxides precipitation is significantly affected by factors such as grain size and the rate of precipitation in addition to pH conditions [130]. The enrichment of ^{56}Fe in the fluid phase at the start of oxidative dissolution of sulfide-rich rocks at pH 2 has been demonstrated [131] (Figure 7a). The initial isotopic enrichment of solution suggested a ^{56}Fe-dominated reservoir of the mineral that was washed into the leachate. The authors of Fernandez and Borrok [131] identified the ^{56}Fe-rich reservoir as a thin layer of ferric-oxide on the sulfide surface that was the result of air oxidation prior to leaching. This transient redox isotope effect was followed by the dominance of kinetic fractionation as more iron was released with time, which decreased the δ^{56}Fe value of the solution. Whilst in the acidic experiments, the influence of the redox-driven, surface-related mechanisms were significant, at pH 5, the precipitation of secondary ferric minerals from the solution controlled the redistribution of Fe isotopes (Figure 7b). Figure 7b shows that during the dissolution of sulfide-rich rocks under circumneutral conditions, the leachate is consistently characterized by lower δ^{56}Fe values compared to bulk rock due to the immediate formation of secondary precipitates [131]. Whereas the aqueous oxidation of Fe^{2+} under acidic abiotic conditions (pH2)–described by the Reaction (5) in Section 2–is limited due to its sluggish kinetics [50], the rapid oxidation of aqueous Fe(II) and the subsequent precipitation of Fe(III) oxyhydroxides is enabled at circumneutral pH values (pH 5). The system reaches the equilibrium isotope fractionation between aqueous Fe(II) and Fe(III) quickly and the precipitated Fe(III) prefers the incorporation of heavy Fe isotopes [127]. This results in a decrease of the Fe isotope ratios in the fluid phase (Figure 7b). Nevertheless, it is important to note that secondary minerals such as jarosite and Fe-(oxy)hydroxides can show lighter Fe isotopic signatures compared to their parent material or the solution under certain conditions [132,133].

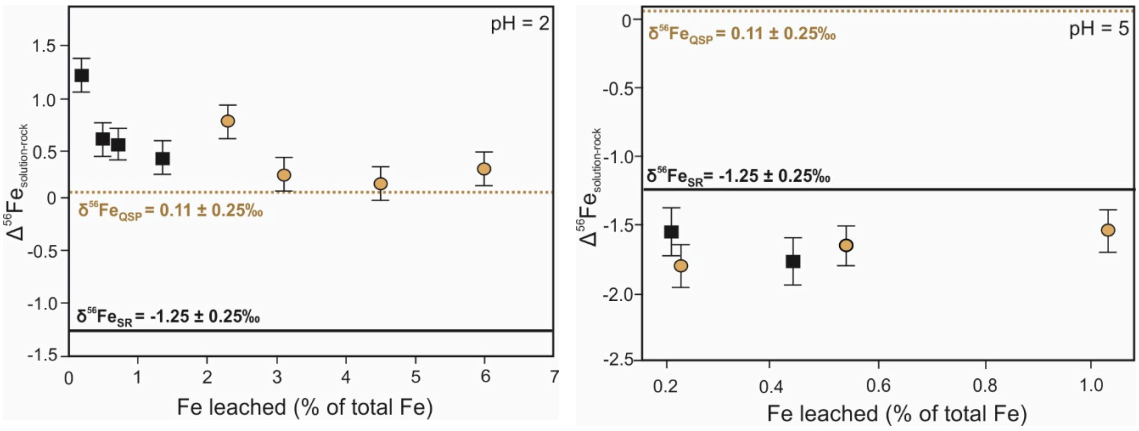

Figure 7. Fractionation of iron isotopes between solution and sulfide-rich rocks ($\Delta_{solution\text{-}rock}$ = $\delta^{56}Fe_{solution} - \delta^{56}Fe_{rock}$) as a function of Fe recovery (**a**) under pH = 2 and (**b**) pH = 5 conditions during continuous batch leaching. Square symbols—leachate of sulfide rock (SR) group: pyrite, chalcopyrite,

galena, sericite, pyrophyllite, anglesite, sphalerite. $\delta^{56}Fe_{SR}$ = –1.25 ± 0.25‰. Circle symbols—leachate of quartz-sericite-pyrite (QSP) group: pyrite, sericite, pyrophyllite, quartz. $\delta^{56}Fe_{QSP}$ = 0.11 ± 0.25‰. Redrawn from Fernandez and Borrok [131].

Influence of Microorganisms on Iron Isotope Fractionation

Various biotic leaching experiments have been performed to investigate the effect of bacterial activity on the isotope fractionation in geological environments [72,134–138]. Microorganisms such as *Acidithiobacillus ferrooxidans* grow in a naturally acidic environment mainly on the surface of different sulfide minerals [139,140]. The *Acidithiobacillus* group of organisms are known for their ability to dissolve transient metals from sulfide minerals by both contact and indirect oxidation [141,142]. Thus, the presence of these bacteria and other microorganisms around sulfide deposits has a potential to accelerate the oxidation that facilitates the increased rates of ARD generation.

Leaching experiments of different iron minerals demonstrate both the presence and absence of bacterial control on Fe isotopes during the dissolution. Although many biological processes are kinetically controlled [28], experimental works indicate ^{56}Fe uptake by microorganisms [143,144]. The assimilation of heavy Fe isotope by bacteria decreases the $\delta^{56}Fe$ value of the solution. The authors of Croal et al. [145] demonstrated 1.5‰ microbial fractionation between aqueous Fe(II) and Fe(III). Based on this result, the biological control on redox processes and subsequent isotope fractionations were suggested. In contrast, the authors of Balci et al. [133] identified abiotically controlled Fe isotope fractionation between Fe(II) and Fe(III) under acidic conditions (pH < 3) for biotic and abiotic oxidation experiments. Bio- and electro-chemical leaching experiments of metal sulfides under consistent redox conditions found no significant difference in Fe isotope fractionation (Figure 8) [138]. This emphasizes the importance of redox potential conditions as the main factor governing the redistribution of Fe isotopes during sulfide dissolution, which seems to be a unique signature of the sulfide system.

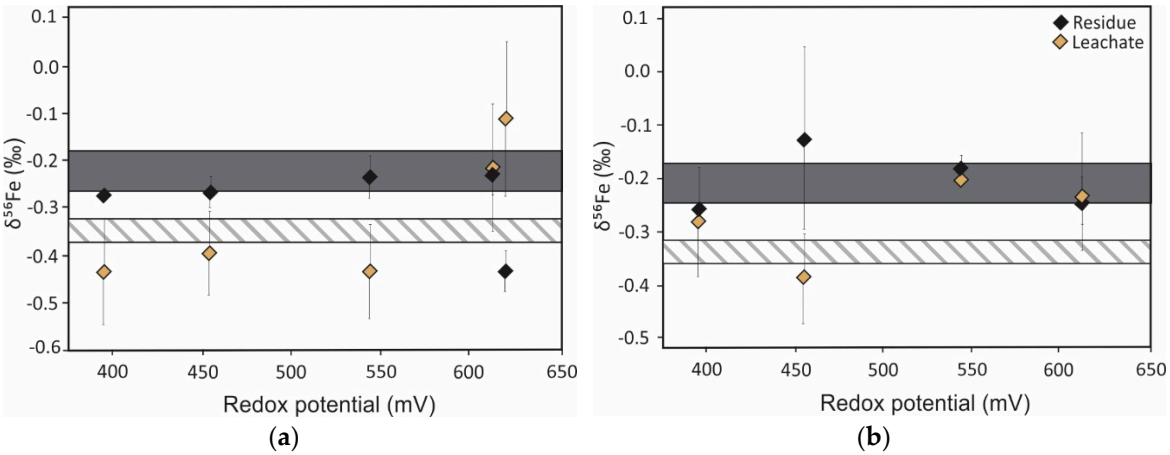

Figure 8. Plot of $\delta^{56}Fe$ values in residues and leachates as a function of redox potential for (**a**) bioleaching and (**b**) electrochemical leaching of pyritic chalcopyrite concentrate. Grey areas represent the initial isotopic composition of the mineral concentrate with 2σ errors. Dashed areas represent the initial isotopic composition of the solution with 2σ errors. Error bars of samples are 2σ. Redrawn from Rodríguez et al. [138].

Concordant Fe isotope variation mechanisms in biotic and abiotic experiments do not allow for the distinction between biological Fe fractionation and that of abiotic chemical reactions, and points to the complexity of controlling mechanisms of various isotope systems even under laboratory conditions. Further investigations that allow for the accurate characterization of abiotic and biotic processes are warranted.

6. Summary and Future Perspective

Pyrite, as the most common sulfide mineral in nature, plays a significant role in directly controlling sulfur and iron cycles and in indirectly controlling the oxygen cycle. The importance of the oxidative dissolution of pyrite relates to its environmental impact through ARD generation. Therefore, an understanding of the processes and mechanisms governing pyrite dissolution facilitates the predictive modelling of ARD, which in turn can be used to inform effective geotechnical designs and rehabilitation strategies. In summary, under controlled laboratory conditions, the use of pure mineral phases allows measurement of the discrete isotope fractionations and therefore the effects of ARD-related processes on different isotope systems can be inferred with greater certainty. Where reactions cannot be controlled due to their coexistence, the closed system in the laboratory enables the recognition of additional mechanisms by retaining the end-products, e.g., SO_2 degassing during the initial dissolution of pyrite. Interpretation of results in the field are therefore strengthened by controlled laboratory experiments that more accurately estimate the discrete fractionation factors that belong to well-defined processes. Sulfur, oxygen, and iron isotope signatures and their key roles in ARD characterization are summarized in Table 1.

Table 1. Summary of the main isotopic signatures during the oxidative leaching of pyrite

Isotope	Process	Isotopic Signature of the Process	Role in ARD Characterization	Notes
Sulfur	Quantitative conversion of pyrite to sulfate	Fractionation ranges between −1.3 ‰ and +0.4 ‰ [63,70–74]	Allows the identification of pyrite as the source of sulfur	Inconsistent sulfate $\delta^{34}S$ values during pyrite dissolution due to SO_2 degassing [78]
	Stepwise or incomplete conversion of pyrite to sulfate	Degree of fractionation varies with the oxidation state of sulfur [72,74,97]	Provide information about the pathways of sulfur oxidation or reduction	^{34}S enrichment follows the general trend: SO_4^{2-} > SO_3^{2-} > $S_2O_3^{2-}$ > S^0 > S^{2-} [96]
Oxygen	Quantitative conversion of pyrite to sulfate	Sulfate $\delta^{18}O$ mainly depends on the relative contribution of oxygen sources [68,109–112]	Indicative of the dominant reaction mechanism that is responsible for pyrite oxidation	Inconsistent sulfate $\delta^{18}O$ values during pyrite dissolution due to prolonged oxygen isotope equilibration [78]
	Stepwise or incomplete conversion of pyrite to sulfate	Sulfate $\delta^{18}O$ is influenced by the presence of sulfur intermediates [61]	Provide insights into intermediate mechanisms that control pyrite oxidation	Oxygen exchange kinetics between sulfur oxyanions and water varies with the oxidation state of sulfur [146]
Iron	Oxidative dissolution of pyrite	Fractionation between $Fe^{2+}{}_{FeS2}$ and $Fe^{3+}{}_{precipitate}$ ranges from −1.7 ‰ to 3.0 ‰ [128,129,131] [1]	Provide insights into source and (bio)geochemical cycling of iron	Inconsistent solution $\delta^{56}Fe$ values at pH 2 due to dissolution of air oxidized layer [131]

[1] Presence of bacteria might affect the iron isotope system by decreasing the $\delta^{56}Fe$ value of the solution due to the uptake of ^{56}Fe [144,145].

Based on the summaries presented here, some potential focus areas for future studies are outlined:

1. Understanding the role of pyrite type: Most laboratory experiments have used hydrothermal pyrite, even though it is well established that pyrites from different geological environments, morphologies, or electrochemical properties [37] show distinctly different oxidation rates and dissolution signatures [147,148]. Consequently, there is a need to extend the database of isotope fractionation factors to include all forms and physical parameters of pyrites in order to apply the most appropriate fractionation factors in field studies.
2. Understanding acid neutralization processes: An understudied but promising area in the application of isotope geochemistry involves the isotope signatures of neutralization processes.

ARD-related carbon isotope fractionation would not only provide information on the mechanisms of neutralization reactions, but also has the potential to determine the relative proportion of the main neutralizing carbonate phases using mixing calculations. This may provide more accurate Acid Neutralizing Capacity (ANC) calculations, as currently calcite is considered as the most dominant neutralizing mineral [3] without its quantified relative contribution to neutralization.

3. Understanding the role of different mineral processing and metallurgical activities on isotope processes: Although several isotope investigations have been undertaken in mining areas to track ARD-related processes in underground and surface water bodies, the method still has not become common practice. In addition, most of these field studies are focused on underground mine workings, pit lakes, as well as waste and water storage facilities that are collectively considered as the major environments of ARD generation. To our knowledge, no studies have examined the role of ore beneficiation processes in ARD formation using the isotope techniques in detail. The water consumption of different processing steps such as milling, dense media separation, or flotation may also provide the required conditions of sulfide oxidation, allowing the initial steps of ARD generation to take place. Tracking the sulfide oxidation pathways and sulfur transformations during various beneficiations steps would help to assess the relative contribution of mineral processing to ARD generation. Eliminating the ARD potential before waste disposal would have a significant beneficial impact on mine water quality. In addition, the quantification of mineral oxidation rates of certain processing steps via isotopes could add to process optimization by the evaluation of more accurate residence times.
4. ARD prevention, mitigation, and management: In order to minimize the potential impacts of ARD on natural water systems, it is necessary to understand (i) the mechanisms taking place during ARD formation and (ii) the mechanisms that control the mobility of contaminants. Although isotopes are successfully used in pollution source-tracking and transportation modelling, the applications of isotopes in ARD generation processes are not yet fully explored. To create more accurate prediction models and thus be able to select the most optimal pollution emission control strategies, more accurate isotope fractionation factors and the identification of causative mechanisms are required. Accurate measurements of fractionation would allow the estimation of various reaction rates with greater certainty. This would help to improve our ability to evaluate the chemical evolution of both mine waste material and the impacted water systems, potentially informing ARD control measures in a timely manner. In addition to tracking ARD generation and transportation, isotopes also can be used in evaluating the effectiveness of different remediation methods, for example, passive treatment systems [75,149].

The application of stable isotopes in environmental studies has a significant potential to facilitate the sustainability in water resources management. Precise quantification of discrete fractionation factors will extend this methodology into new areas and has implications in describing complex natural systems with greater certainty.

Author Contributions: Conceptualization, M.B., J.B., S.T.L.H. and Á.Ó.; validation, M.B., M.E. and S.T.L.H.; writing—original draft preparation, Á.Ó.; writing—review and editing, Á.Ó., M.B., M.E., J.B. and S.T.L.H.; visualization, Á.Ó.; supervision, M.B.; funding acquisition, S.T.L.H. and J.B. All authors have read and agreed to the published version of the manuscript.

Funding: National Research Foundation of South Africa (NRF)-South African Research Chairs Initiative (SARChI Chair in Minerals Beneficiation), UID 64829.

Acknowledgments: We thank Chris Harris for his helpful comments on this manuscript. This work is based on research supported by the National Research Foundation of South Africa (NRF) through their South African Research Chairs Initiative (SARChI Chair in Minerals Beneficiation, held by Jochen Petersen, UID 64829). Any opinion, finding, conclusions, or recommendation expressed in this material is that of the authors and the NRF does not accept any liability in this regard. The three anonymous reviewers and Carlito Tabelin are thanked for their constructive reviews that substantially improved this paper.

Conflicts of Interest: The authors declare no conflict of interest.

References

1. Egiebor, N.O.; Oni, B. Acid Rock Drainage Formation and Treatment: A Review. *Asia Pac. J. Chem. Eng.* **2007**, *2*, 47–62. [CrossRef]
2. Moncur, M.C.; Jambor, J.L.; Ptacek, C.J.; Blowes, D.W. Mine Drainage from the Weathering of Sulfide Minerals and Magnetite. *Appl. Geochem.* **2009**, *24*, 2362–2373. [CrossRef]
3. Dold, B. Basic Concepts in Environmental Geochemistry of Sulfidic Mine-Waste Management. In *Waste Management*; Kumar, E.S., Ed.; InTech: Rijeka, Croatia, 2010. Available online: http://www.intechopen.com/books/waste-management/basic-concepts-in-environmental-geochemistry-ofsulfidic-mine-waste-management (accessed on 22 May 2020).
4. Chopard, A.; Benzaazoua, M.; Bouzahzah, H.; Plante, B.; Marion, P. A Contribution to Improve the Calculation of the Acid Generating Potential of Mining Wastes. *Chemosphere* **2017**, *175*, 97–107. [CrossRef]
5. Akcil, A.; Koldas, S. Acid Mine Drainage (AMD): Causes, Treatment and Case Studies. *J. Clean. Prod.* **2006**, *14*, 1139–1145. [CrossRef]
6. Larsen, D.; Mann, R. Origin of High Manganese Concentrations in Coal Mine Drainage, Eastern Tennessee. *J. Geochem. Explor.* **2005**, *86*, 143–163. [CrossRef]
7. Cravotta, C.A. Dissolved Metals and Associated Constituents in Abandoned Coal-Mine Discharges, Pennsylvania, USA. Part 1: Constituent Quantities and Correlations. *Appl. Geochem.* **2008**, *23*, 166–202. [CrossRef]
8. Vyawahre, A.; Rai, S. Acid Mine Drainage: A Case Study of An Indian Coal Mine. *Int. J. Sci. Res. Sci. Eng. Technol.* **2016**, *2*, 1297–1301.
9. Bell, F.G.; Bullock, S.E.T.; Hälbich, T.F.; Lindsay, P. Environmental Impacts Associated with an Abandoned Mine in The Witbank Coalfield, Sout Africa. *Int. J. Coal Geol.* **2001**, *45*, 195–216. [CrossRef]
10. Casiot, C.; Egal, M.; Elbaz-Poulichet, F.; Bruneel, O.; Bancon-Montigny, C.; Cordier, M.-A.; Gomez, E.; Aliaume, C. Hydrological and Geochemical Control of Metals and Arsenic in a Mediterranean River Contaminated by Acid Mine Drainage (the Amous River, France); Preliminary Assessment of Impacts on Fish (*Leuciscus Cephalus*). *Appl. Geochem.* **2009**, *24*, 787–799. [CrossRef]
11. Olenici, A.; Blanco, S.; Borrego-Ramos, M.; Momeu, L.; Baciu, C. Exploring the Effects of Acid Mine Drainage on Diatom Teratology Using Geometric Morphometry. *Ecotoxicology* **2017**, *26*, 1018–1030. [CrossRef]
12. Vega, F.A.; Covelo, E.F.; Andrade, M.L. Competitive Sorption and Desorption of Heavy Metals in Mine Soils: Influence of Mine Soil Characteristics. *J. Colloid Interface Sci.* **2006**, *298*, 582–592. [CrossRef] [PubMed]
13. Bååth, E.; Anderson, T.-H. Comparison of Soil Fungal/Bacterial Ratios in a PH Gradient Using Physiological and PLFA-Based Techniques. *Soil Biol. Biochem.* **2003**, *35*, 955–963. [CrossRef]
14. Rodríguez, L.; Ruiz, E.; Alonso-Azcárate, J.; Rincón, J. Heavy Metal Distribution and Chemical Speciation in Tailings and Soils around a Pb–Zn Mine in Spain. *J. Environ. Manag.* **2009**, *90*, 1106–1116. [CrossRef] [PubMed]
15. Skousen, J.; Zipper, C.E.; Rose, A.; Ziemkiewicz, P.F.; Nairn, R.; McDonald, L.M.; Kleinmann, R.L. Review of Passive Systems for Acid Mine Drainage Treatment. *Mine Water Environ.* **2017**, *36*, 133–153. [CrossRef]
16. Clarke, L.B. *Coal Mining and Water Quality*; Technical Report; IEA Coal Research: London, UK, 1995.
17. Jambor, J.L.; Nordstrom, D.K.; Alpers, C.N. Metal-Sulfate Salts from Sulfide Mineral Oxidation. *Rev. Mineral. Geochem.* **2000**, *40*, 303–350. [CrossRef]
18. Nicholson, R.Y. Iron-Sulfide Oxidation Mechanisms; Laboratory Studies. In *The Environmental Geochemistry of Sulfide, Mine-Wastes*; Short Course Handbook; Blowes, D.W., Jambor, J.L., Eds.; Mineralogical Association of Canada: Nepean, ON, Canada, 1994; Volume 22, pp. 163–183.
19. Chandra, A.P.; Gerson, A.R. The Mechanisms of Pyrite Oxidation and Leaching: A Fundamental Perspective. *Surf. Sci. Rep.* **2010**, *65*, 293–315. [CrossRef]
20. Tabelin, C.B.; Corpuz, R.D.; Igarashi, T.; Villacorte-Tabelin, M.; Alorro, R.D.; Yoo, K.; Raval, S.; Ito, M.; Hiroyoshi, N. Acid Mine Drainage Formation and Arsenic Mobility under Strongly Acidic Conditions: Importance of Soluble Phases, Iron Oxyhydroxides/Oxides and Nature of Oxidation Layer on Pyrite. *J. Hazard. Mater.* **2020**, *399*, 122844. [CrossRef]
21. Dold, B. Evolution of Acid Mine Drainage Formation in Sulphidic Mine Tailings. *Minerals* **2014**, *4*, 621–641. [CrossRef]

22. Parbhakar-Fox, A.; Lottermoser, B.G. A Critical Review of Acid Rock Drainage Prediction Methods and Practices. *Miner. Eng.* **2015**, *82*, 107–124. [CrossRef]
23. Dold, B. Acid Rock Drainage Prediction: A Critical Review. *J. Geochem. Explor.* **2017**, *172*, 120–132. [CrossRef]
24. Brady, K.B.C.; Perry, E.F.; Beam, R.L.; Bisko, D.C.; Gardner, M.D.; Tarantino, J.M. Evaluation of Acid-Base Accounting to Predict the Quality of Drainage at Surface Coal Mines in Pennsylvania, U.S.A. *J. Am. Soc. Min. Reclam.* **1994**, *1*, 138–147. [CrossRef]
25. Paktunc, A.D. Mineralogical Constraints on the Determination of Neutralization Potential and Prediction of Acid Mine Drainage. *Environ. Geol.* **1999**, *39*, 103–112. [CrossRef]
26. Verburg, R.; Bezuidenhout, N.; Chatwin, T.; Ferguson, K. The Global Acid Rock Drainage Guide (GARD Guide). *Mine Water Environ.* **2009**, *28*, 305–310. [CrossRef]
27. Morin, K.A.; Hutt, N.M.; Ferguson, K.D. Measured Rates of Sulfide Oxidation and Neutralization in Kinetic Tests: Statistical Lessons from the Database. In Proceedings of the Sudbury '95: Mining and the Environment, Sudbury, ON, Canada, 23 May–1 June 1995; pp. 525–536.
28. Banerjee, D. Acid Drainage Potential from Coal Mine Wastes: Environmental Assessment through Static and Kinetic Tests. *Int. J. Environ. Sci. Technol.* **2014**, *11*, 1365–1378. [CrossRef]
29. Tabelin, C.B.; Igarashi, T.; Villacorte-Tabelin, M.; Park, I.; Opiso, E.M.; Ito, M.; Hiroyoshi, N. Arsenic, Selenium, Boron, Lead, Cadmium, Copper, and Zinc in Naturally Contaminated Rocks: A Review of Their Sources, Modes of Enrichment, Mechanisms of Release, and Mitigation Strategies. *Sci. Total Environ.* **2018**, *645*, 1522–1553. [CrossRef]
30. Becker, M.; Dyantyi, N.; Broadhurst, J.L.; Harrison, S.T.L.; Franzidis, J.P. A Mineralogical Approach to Evaluating Laboratory Scale Acid Rock Drainage Characterisation Tests. *Miner. Eng.* **2015**, *80*, 33–36. [CrossRef]
31. Jamieson, H.E.; Walker, S.R.; Parsons, M.B. Mineralogical Characterization of Mine Waste. *Appl. Geochem.* **2015**, *57*, 85–105. [CrossRef]
32. Guseva, O.; Opitz, A.; Broadhurst, J.; Harrison, S.; Becker, M. Characterisation and prediction of acid rock drainage in waste rock: Value of integrating quantitative mineralogical and textural measurements. *Miner. Eng*. Under review.
33. Moodley, I.; Sheridan, C.M.; Kappelmeyer, U.; Akcil, A. Environmentally Sustainable Acid Mine Drainage Remediation: Research Developments with a Focus on Waste/by-Products. *Miner. Eng.* **2018**, *126*, 207–220. [CrossRef]
34. Abraitis, P.K.; Pattrick, R.A.D.; Vaughan, D.J. Variations in the Compositional, Textural and Electrical Properties of Natural Pyrite: A Review. *Int. J. Miner. Process.* **2004**, *74*, 41–59. [CrossRef]
35. Savage, K.S.; Stefan, D.; Lehner, S.W. Impurities and Heterogeneity in Pyrite: Influences on Electrical Properties and Oxidation Products. *Appl. Geochem.* **2008**, *23*, 103–120. [CrossRef]
36. Tabelin, C.B.; Igarashi, T.; Tamoto, S.; Takahashi, R. The Roles of Pyrite and Calcite in the Mobilization of Arsenic and Lead from Hydrothermally Altered Rocks Excavated in Hokkaido, Japan. *J. Geochem. Explor.* **2012**, *119–120*, 17–31. [CrossRef]
37. Lotter, N.O.; Bradshaw, D.J.; Barnes, A.R. Classification of the Major Copper Sulphides into Semiconductor Types, and Associated Flotation Characteristics. *Miner. Eng.* **2016**, *96–97*, 177–184. [CrossRef]
38. Miljević, N.; Golobočanin, D. Potential Use of Environmental Isotopes in Pollutant Migration Studies. *Arh. Hig. Rada Toksikol.* **2007**, *58*, 251–262. [CrossRef]
39. Wiederhold, J.G. Metal Stable Isotope Signatures as Tracers in Environmental Geochemistry. *Environ. Sci. Technol.* **2015**, *49*, 2606–2624. [CrossRef]
40. Seal, R.R.; Alpers, C.N.; Rye, R.O. Stable Isotope Systematics of Sulfate Minerals. *Rev. Mineral. Geochem.* **2000**, *40*, 541–602. [CrossRef]
41. Skierszkan, E.; Mayer, U.; Beckie, R.; Weis, D. Tracking the Fate of Metals in Mining Waste Rock Using Metal Stable Isotopes. In Proceedings of the Agreeing on Solutions for more Sustainable Mine Water Management, 10th International Conference on Acid Rock Drainage and IMWA Annual Conference, Santiago, Chile, 21–24 April 2015; Brown, A., Bucknam, C., Burgess, J., Carballo, M., Castendyk, D., Figueroa, L., Kirk, L., McLemore, V., McPhee, J., O'Kane, M., et al., Eds.; p. 236.
42. Michener, R.H.; Lajtha, K. *Stable Isotopes in Ecology and Environmental Science*, 2nd ed.; Blackwell Publishing Ltd.: Oxford, UK, 2007; pp. 6–11.

43. Weiss, D.J.; Rehkämper, M.; Schoenberg, R.; McLaughlin, M.; Kirby, J.; Campbell, P.G.C.; Arnold, T.; Chapman, J.; Peel, K.; Gioia, S. Application of Non-traditional Stable-isotope Systems to the Study of Sources and Fate of Metals in the Environment. *Environ. Sci. Technol.* **2008**, *42*, 655–664. [CrossRef]
44. Young, E.D.; Galy, A.; Nagahara, H. Kinetic and Equilibrium Mass-dependent Isotope Fractionation Laws in Nature and Their Geochemical and Cosmochemical Significance. *Geochim. Cosmochim. Acta* **2002**, *66*, 1095–1104. [CrossRef]
45. Sharp, Z. *Principles of Stable Isotope Geochemistry*, 2nd ed.; Pearson Education: Upper Saddle River, NJ, USA, 2017.
46. Garrels, R.; Thompson, M. Oxidation of Pyrite by Iron Sulfate Solutions. *Am. J. Sci.* **1960**, *258*, 57–67.
47. Nordstrom, K.D.; Alpers, C.N. Geochemistry of Acid Mine Waters. In *The Environmental Geochemistry of Mineral Deposits. Part A: Processes, Techniques, and Health Issues*; Plumlee, G.D., Logsdon, M.J., Filipek, L.F., Eds.; Society of Economic Geologists: Littleton, CO, USA, 1999; Volume 6, pp. 133–160.
48. Smart, M.; Huddy, R.J.; Edward, C.J.; Fourie, C.; Shumba, T.; Iron, J.; Harrison, S.T.L. Linking Microbial Community Dynamics in BIOX® Leaching Tanks to Process Conditions: Integrating Lab and Commercial Experience. *Solid State Phenom.* **2017**, *262*, 38–42. [CrossRef]
49. Tupikina, O.V.; Minnaar, S.H.; van Hille, R.P.; van Wyk, N.; Rautenbach, G.F.; Dew, D.; Harrison, S.T.L. Determining the Effect of Acid Stress on the Persistence and Growth of Thermophilic Microbial Species after Mesophilic Colonisation of Low Grade Ore in a Heap Leach Environment. *Miner. Eng.* **2013**, *53*, 152–159. [CrossRef]
50. Nordstrom, K.D.; Southam, G. Geomicrobiology of Sulfide Mineral Oxidation. In *Geomicrobiology: Interactions between Microbes and Minerals: Reviews in Mineralogy*; Banfield, J.F., Nealson, K.H., Eds.; Mineralogical Society of America: Washington, DC, USA, 1997; Volume 35, pp. 361–390.
51. Mustin, C.; Berthelin, J.; Marion, P.; de Donato, P. Corrosion and Electrochemical Oxidation of a Pyrite by Thiobacillus ferrooxidans. *Appl. Environ. Microbiol.* **1992**, *58*, 1175–1182. [CrossRef]
52. Rimstidt, D.D.; Vaughan, D.J. Pyrite Oxidation: A State-of-the-Art Assessment of the Reaction Mechanism. *Geochim. Cosmochim. Acta* **2003**, *67*, 873–880. [CrossRef]
53. Moses, C.O.; Herman, J.S. Pyrite Oxidation at Circumneutral pH. *Geochim. Cosmochim. Acta* **1991**, *55*, 471–482. [CrossRef]
54. Kelsall, G.H.; Yin, Q.; Vaughan, D.J.; England, K.E.R.; Brandon, N.P. Electrochemical Oxidation of Pyrite (FeS2) in Aqueous Electrolytes. *J. Electroanal. Chem.* **1999**, *471*, 116–125. [CrossRef]
55. Tabelin, C.B.; Veerawattananun, S.; Ito, M.; Hiroyoshi, N.; Igarashi, T. Pyrite Oxidation in the Presence of Hematite and Alumina: II. Effects on the Cathodic and Anodic Half-Cell Reactions. *Sci. Total Environ.* **2017**, *581–582*, 126–135. [CrossRef]
56. Tu, Z.; Wan, J.; Guo, C.; Fan, C.; Zhang, T.; Lu, G.; Reinfelder, J.R.; Dang, Z. Electrochemical Oxidation of Pyrite in PH 2 Electrolyte. *Electrochim. Acta* **2017**, *239*, 25–35. [CrossRef]
57. Li, X.; Gao, M.; Hiroyoshi, N.; Tabelin, C.B.; Taketsugu, T.; Ito, M. Suppression of Pyrite Oxidation by Ferric-Catecholate Complexes: An Electrochemical Study. *Miner. Eng.* **2019**, *138*, 226–237. [CrossRef]
58. Nourmohamadi, H.; Aghazadeh, V.; Esrafili, M.D. A Comparative DFT Study of Fe^{3+} and Fe^{2+} Ions Adsorption on (100) and (110) Surfaces of Pyrite: An Electrochemical Point of View. *Surf. Interface Anal.* **2020**, *52*, 110–118. [CrossRef]
59. Jerz, J.K.; Rimstidt, J.D. Pyrite Oxidation in Moist Air. Geochim. *Cosmochim. Acta* **2004**, *68*, 701–714. [CrossRef]
60. Borda, M.J.; Strongin, D.R.; Schoonen, M.A.A. Vibrational Spectroscopic Study of Pyrite Oxidation. *Am. Mineral.* **2003**, *88*, 1318–1323. [CrossRef]
61. Nordstrom, K.D.; Wright, W.G.; Mast, A.M.; Bove, D.J.; Rye, R.O. Aqueous-Sulfate Stable Isotopes-A Study of Mining-Affected and Undisturbed Acidic Drainage. In *Integrated Investigations of Environmental Effects of Historical Mining in the Animas River Watershed, San Juan County, Colorado*; Church, S.E., von Guerard, P., Finger, S.E., Eds.; U.S. Geological Survey Professional Paper 1651; USGS: Lawrence, KS, USA, 2007; Volume 1, pp. 387–416.
62. Field, C.W. Sulfur Isotopic Method for Discriminating between Sulfates of Hypogene and Supergene Origin. *Econ. Geol.* **1966**, *61*, 1428–1435. [CrossRef]
63. Taylor, B.E.; Wheeler, M.C.; Nordstrom, D.K. Stable Isotope Geochemistry of Acid Mine Drainage: Experimental Oxidation of Pyrite. *Geochim. Cosmochim. Acta* **1984**, *48*, 2669–2678. [CrossRef]

64. Taylor, B.E.; Wheeler, M.C. Sulfur- and Oxygen-isotope Geochemistry of Acid Mine Drainage in the Western United States. In *Environmental Geochemistry of Sulfide Oxidation*; Alpers, C.N., Blowes, D.W., Eds.; American Chemical Society Symposium Series: Washington, DC, USA, 1993; Volume 550, pp. 481–514.
65. Van Stempvoort, D.R.; Krouse, H.R. Controls of $\delta^{18}O$ in Sulfate: Review of Experimental Data and Application to Specific Environments. In *Environmental Geochemistry of Sulfide Oxidation*; Alpers, C.N., Blowes, D.W., Eds.; American Chemical Society Symposium Series: Washington, DC, USA, 1993; Volume 550, pp. 446–480.
66. Krouse, H.R.; Mayer, B. Sulphur and Oxygen Isotopes in Sulphate. In *Environmental Tracers in Subsurface Hydrology*; Cook, P., Herczeg, A., Eds.; Kluwer Academic Publishers: Dordrecht, The Netherlands, 2000; pp. 195–231.
67. Otero, N.; Soler, A.; Canals, À. Controls of $\delta^{34}S$ and $\delta^{18}O$ in Dissolved Sulphate: Learning from a Detailed Survey in the Llobregat River (Spain). *Appl. Geochem.* **2008**, *23*, 1166–1185. [CrossRef]
68. Migaszewski, Z.M.; Gałuszka, A.; Hałas, S.; Dołęgowska, S.; Dabek, J.; Starnawska, E. Geochemistry and Stable Sulfur and Oxygen Isotope Ratios of the Podwiśniówka Pit Pond Water Generated by Acid Mine Drainage (Holy Cross Mountains, South-Central Poland). *Appl. Geochem.* **2008**, *23*, 3620–3634. [CrossRef]
69. Migaszewski, Z.M.; Gałuszka, A.; Michalik, A.; Dołęgowska, S.; Migaszewski, A.; Hałas, S.; Trembaczowski, A. The Use of Stable Sulfur, Oxygen and Hydrogen Isotope Ratios as Geochemical Tracers of Sulfates in the Podwiśniówka Acid Drainage Area (South-Central Poland). *Aquat. Geochem.* **2013**, *19*, 261–280. [CrossRef]
70. Nakai, N.; Jensen, M.L. The Kinetic Isotope Effect in the Bacterial Reduction and Oxidation of Sulfur. *Geochim. Cosmochim. Acta* **1964**, *28*, 1893–1912. [CrossRef]
71. McCready, R.G.L.; Krouse, H.R. Sulfur Isotope Fractionation during the Oxidation of Elemental Sulfur by Thiobacilli in a Solonetzic Soil. *Can. J. Soil Sci.* **1982**, *62*, 105–110. [CrossRef]
72. Balci, N.; Shanks, W.C.; Mayer, B.; Mandernack, K.W. Oxygen and Sulfur Isotope Systematics of Sulfate Produced by Bacterial and Abiotic Oxidation of Pyrite. *Geochim. Cosmochim. Acta* **2007**, *71*, 3796–3811. [CrossRef]
73. Pisapia, C.; Chaussidon, M.; Mustin, C.; Humbert, B. O and S Isotopic Composition of Dissolved and Attached Oxidation Products of Pyrite by *Acidithiobacillus ferrooxidans*: Comparison with Abiotic Oxidations. *Geochim. Cosmochim. Acta* **2007**, *71*, 2474–2490. [CrossRef]
74. Heidel, C.; Tichomirowa, M. The Isotopic Composition of Sulfate from Anaerobic and Low Oxygen Pyrite Oxidation Experiments with Ferric Iron—New Insights into Oxidation Mechanisms. *Chem. Geol.* **2011**, *281*, 305–316. [CrossRef]
75. Lefticariu, L.; Behum, P.; Bender, K.; Lefticariu, M. Sulfur Isotope Fractionation as an Indicator of Biogeochemical Processes in an AMD Passive Bioremediation System. *Minerals* **2017**, *7*, 41. [CrossRef]
76. Alvaro, A.; Roldán, F.V. Stable Isotope Composition of Acid Mine Drainage Minerals from San Miguel Massive Sulphide Mine Waste. In Proceedings of the Securing the Future: Mining, Metals and the Environment in a Sustainable Society, 8th International Conference on Acid Rock Drainage, Skellefteå, Sweden, 22–26 June 2009; pp. 166–176.
77. Gallo, A.A.; Roldán, F.V. Stable Isotope Study in Iron-Rich Sulphates from San Miguel Mine Wastes (Iberian Pyrite Belt, Spain). *Rev. Soc. Española Mineral.* **2009**, *11*, 27–28.
78. Brunner, B.; Yu, J.Y.; Mielke, R.E.; MacAskill, J.A.; Madzunkov, S.; McGenity, T.J.; Coleman, M. Different Isotope and Chemical Patterns of Pyrite Oxidation Related to Lag and Exponential Growth Phases of *Acidithiobacillus ferrooxidans* Reveal a Microbial Growth Strategy. *Earth Planet. Sci. Lett.* **2008**, *270*, 63–72. [CrossRef]
79. Yu, J.Y.; McGenity, T.J.; Coleman, M.L. Solution Chemistry during the Lag Phase and Exponential Phase of Pyrite Oxidation by *Thiobacillus ferrooxidans*. *Chem. Geol.* **2001**, *175*, 307–317. [CrossRef]
80. Descostes, M.; Vitorge, P.; Beaucaire, C. Pyrite Dissolution in Acidic Media. *Geochim. Cosmochim. Acta* **2004**, *68*, 4559–4569. [CrossRef]
81. Granger, H.C.; Warren, C.G. Unstable Sulfur Compounds and the Origin of Roll-Type Uranium Deposits. *Econ. Geol.* **1969**, *64*, 160–171. [CrossRef]
82. Basolo, F.; Pearson, R.G. *Mechanisms of Inorganic Reactions—A Study of Metal Complexes in Solution*, 2nd ed.; John Wiley and Sons Ltd.: New York, NY, USA, 1967.
83. Goldhaber, M.B. Experimental Study of Metastable Sulfur Oxyanion Formation during Pyrite Oxidation at pH 6–9 and 30 °C. *Am. J. Sci.* **1983**, *283*, 193–217. [CrossRef]
84. Schippers, A.; Jozsa, P.G.; Sand, W. Sulfur Chemistry in the Leaching of Pyrite. *Appl. Environm. Microbiol.* **1996**, *62*, 3424–3431. [CrossRef]

85. Toran, L.; Harris, R.F. Interpretation of Sulfur and Oxygen Isotopes in Biological and Abiological Sulfide Oxidation. *Geochim. Cosmochim. Acta* **1989**, *53*, 2341–2348. [CrossRef]
86. McKibben, M.A.; Barnes, H.L. Oxidation of Pyrite in Low Temperature Acidic Solutions: Rate Laws and Surface Textures. *Geochim. Cosmochim. Acta* **1986**, *50*, 1509–1520. [CrossRef]
87. Luther, G.W. Pyrite Oxidation and Reduction: Molecular Orbital Theory Considerations. *Geochim. Cosmochim. Acta* **1987**, *51*, 3193–3199. [CrossRef]
88. Moses, C.O.; Nordstrom, K.D.; Herman, J.S.; Mills, A.L. Aqueous Pyrite Oxidation by Dissolved Oxygen and by Ferric Iron. *Geochim. Cosmochim. Acta* **1987**, *51*, 1561–1571. [CrossRef]
89. Demoisson, F.; Mullet, M.; Humbert, B. Pyrite Oxidation in Acidic Medium: Overall Reaction Pathway. *Surf. Interface Anal.* **2008**, *40*, 343–348. [CrossRef]
90. Schippers, A.; Sand, W. Bacterial Leaching of Metal Sulfides Proceeds by Two Indirect Mechanisms via Thiosulfate or via Polysulfides and Sulfur. *Appl. Environ. Microbiol.* **1999**, *65*, 319–321. [CrossRef]
91. Sand, W.; Gehrke, T.; Jozsa, P.G.; Schippers, A. (Bio)Chemistry of Bacterial Leaching—Direct vs. Indirect Bioleaching. *Hydrometallurgy* **2001**, *59*, 159–175. [CrossRef]
92. Rohwerder, T.; Gehrke, T.; Kinzler, K.; Sand, W. Bioleaching Review Part A: Progress in bioleaching: Fundamentals and mechanisms of bacterial metal sulfide oxidation. *Appl. Microbiol. Biotechnol.* **2003**, *63*, 239–248. [CrossRef]
93. Borda, M.J.; Elsetinow, A.R.; Strongin, D.R.; Schoonen, M.A.A. Mechanism for the Production of Hydroxyl Radical at Surface Defect Sites on Pyrite. *Geochim. Cosmochim. Acta* **2003**, *67*, 935–939. [CrossRef]
94. Druschel, G.; Borda, M. Comment on "Pyrite Dissolution in Acidic Media" by M. Descostes, P. Vitorge, and C. Beaucaire. *Geochim. Cosmochim. Acta* **2006**, *70*, 5246–5250. [CrossRef]
95. Krouse, H.R.; McCready, R.G.L. Reductive Reactions in the Sulfur Cycle. In *Biochemical Cycling of Mineral-Forming Elements*, 1st ed.; Trudinger, P., Swaine, D., Eds.; Elsevier Science: Amsterdam, The Netherlands, 1979; Volume 3, pp. 315–368.
96. Edraki, M.; Golding, S.D.; Baublys, K.A.; Lawrence, M.G. Hydrochemistry, Mineralogy and Sulfur Isotope Geochemistry of Acid Mine Drainage at the Mt. Morgan Mine Environment, Queensland, Australia. *Appl. Geochem.* **2005**, *20*, 789–805. [CrossRef]
97. Canfield, D.; Thamdrup, B. The Production of ^{34}S-Depleted Sulfide during Bacterial Disproportionation of Elemental Sulfur. *Science* **1994**, *266*, 1973–1975. [CrossRef]
98. Böttcher, M.E.; Thamdrup, B.; Vennemann, T.W. Oxygen and Sulfur Isotope Fractionation during Anaerobic Bacterial Disproportionation of Elemental Sulfur. *Geochim. Cosmochim. Acta* **2001**, *65*, 1601–1609. [CrossRef]
99. Balci, N.; Brunner, B.; Turchyn, A.V. Tetrathionate and Elemental Sulfur Shape the Isotope Composition of Sulfate in Acid Mine Drainage. *Front. Microbiol.* **2017**, *8*, 1564. [CrossRef]
100. Müller, I.A.; Brunner, B.; Coleman, M. Isotopic Evidence of the Pivotal Role of Sulfite Oxidation in Shaping the Oxygen Isotope Signature of Sulfate. *Chem. Geol.* **2013**, *354*, 186–202. [CrossRef]
101. Kokh, M.A.; Assayag, N.; Mounic, S.; Cartigny, P.; Gurenko, A.; Pokrovski, G.S. Multiple Sulfur Isotope Fractionation in Hydrothermal Systems in the Presence of Radical Ions and Molecular Sulfur. *Geochim. Cosmochim. Acta* **2020**, *285*, 100–128. [CrossRef]
102. Lloyd, R.M. Oxygen Isotope Behavior in the Sulfate-Water System. *J. Geophys. Res.* **1968**, *73*, 6099–6110. [CrossRef]
103. Chiba, H.; Sakai, H. Oxygen Isotope Exchange Rate between Dissolved Sulfate and Water at Hydrothermal Temperatures. *Geochim. Cosmochim. Acta* **1985**, *49*, 993–1000. [CrossRef]
104. Seal, R.R.; Wandless, G.A. Sulfur Isotope Evidence for Sea-floor Mineralizing Processes at the Bald Mountain and Mount Chase Massive Sulfide Deposits, Northern Maine. In *Massive Sulfide Deposits of the Bathurst Mining Camp, New Brunswick, and Northern Maine*; Goodfellow, W.D., McCutcheon, S.R., Peter, J.M., Eds.; Society of Economic Geologists: Littleton, CO, USA, 2003; Volume 11, pp. 567–587.
105. Dole, M.; Lane, G.A.; Rudd, D.P.; Zaukelies, D.A. Isotopic Composition of Atmospheric Oxygen and Nitrogen. *Geochim. Cosmochim. Acta* **1954**, *6*, 65–78. [CrossRef]
106. Kroopnick, P.; Craig, H. Atmospheric Oxygen: Isotopic Composition and Solubility Fractionation. *Science* **1972**, *175*, 54–55. [CrossRef]
107. Van Everdingen, R.O.; Krouse, H.R. Isotope Composition of Sulphates Generated by Bacterial and Abiological Oxidation. *Nature* **1985**, *315*, 395–396. [CrossRef]

108. Epstein, S.; Mayeda, T. Variations in the ^{18}O Content of Waters from Natural Sources. *Geochim. Cosmochim. Acta* **1953**, *4*, 213–224. [CrossRef]
109. Rose, A.W.; Cravotta, C.A. Geochemistry of Coal Mine Drainage. In *Coal Mine Drainage Prediction and Pollution Prevention in Pennsylvania*; Brady, K.B.C., Smith, M.W., Schueck, J., Eds.; Pennsylvania Department of Environmental Protection: Harrisburg, PA, USA, 1998; pp. 1.1–1.22.
110. Gammons, C.H.; Duaime, T.E.; Parker, S.R.; Poulson, S.R.; Kennelly, P. Geochemistry and Stable Isotope Investigation of Acid Mine Drainage Associated with Abandoned Coal Mines in Central Montana, USA. *Chem. Geol.* **2010**, *269*, 100–112. [CrossRef]
111. Salifu, M.; Aiglsperger, T.; Mörth, C.-M.; Alakangas, L. Stable Sulphur and Oxygen Isotopes as Indicators of Sulphide Oxidation Reaction Pathways and Historical Environmental Conditions in a Cu–W–F Skarn Tailings Piles, South-Central Sweden. *Appl. Geochem.* **2019**, *110*, 104426. [CrossRef]
112. Butler, T.W. Isotope Geochemistry of Drainage from an Acid Mine Impaired Watershed, Oakland, California. *Appl. Geochem.* **2007**, *22*, 1416–1426. [CrossRef]
113. Qureshi, R.M. The Isotopic Composition of Aqueous Sulfate (A Laboratory Investigation). Ph.D. Thesis, University of Waterloo, Waterloo, ON, Canada, 1986.
114. Sasaki, K.; Tsunekawa, M.; Ohtsuka, T.; Konno, H. Confirmation of a Sulfur-rich Layer on Pyrite after Oxidative Dissolution by Fe(III) Ions around pH2. *Geochim. Cosmochim. Acta* **1995**, *59*, 3155–3158. [CrossRef]
115. Krouse, H.R.; Gould, W.D.; McCready, R.G.L.; Rajan, S. ^{18}O Incorporation into Sulphate during the Bacterial Oxidation of Sulphide Minerals and the Potential for Oxygen Isotope Exchange between O_2, H_2O and Oxidized Sulphur Intermediates. *Earth Planet. Sci. Lett.* **1991**, *107*, 90–94. [CrossRef]
116. Holt, B.D.; Kumar, R.; Cunningham, P.T. Oxygen-18 Study of the Aqueous-Phase of Sulfur Dioxide. *Atmos. Environ.* **1981**, *15*, 557–566. [CrossRef]
117. Viers, J.; Grande Gil, J.A.; Zouiten, C.; Freydier, R.; Masbou, J.; Valente, T.; de la Torre, M.L.; Destrigneville, C.; Pokrovsky, O.S. Are Cu Isotopes a Useful Tool to Trace Metal Sources and Processes in Acid Mine Drainage (AMD) Context? *Chemosphere* **2018**, *193*, 1071–1079. [CrossRef]
118. Zhu, X.K.; Guo, Y.; Williams, R.J.P.; O'Nions, R.K.; Matthews, A.; Belshaw, N.S.; Salvato, B. Mass Fractionation Processes of Transition Metal Isotopes. *Earth Planet. Sci. Lett.* **2002**, *200*, 47–62. [CrossRef]
119. Ehrlich, S.; Butler, I.; Halicz, L.; Rickard, D.; Oldroyd, A.; Matthews, A. Experimental Study of the Copper Isotope Fractionation between Aqueous Cu(II) and Covellite, CuS. *Chem. Geol.* **2004**, *209*, 259–269. [CrossRef]
120. Fantle, M.S.; De Paolo, D.J. Iron Isotopic Fractionation during Continental Weathering. *Earth Planet. Sci. Lett.* **2004**, *228*, 547–562. [CrossRef]
121. Borrok, D.M.; Nimick, D.A.; Wanty, R.B.; Ridley, W.I. Isotopic Variations of Dissolved Copper and Zinc in Stream Waters Affected by Historical Mining. *Geochim. Cosmochim. Acta* **2008**, *72*, 329–344. [CrossRef]
122. Calmano, W.; Hong, J.; Forstner, U. Binding and Mobilization of Heavy Metals in Contaminated Sediments Affected by PH and Redox Potential. *Water Sci. Technol.* **1993**, *28*, 223–235. [CrossRef]
123. Bourg, A.C.M.; Loch, J.P.G. Mobilization of Heavy Metals as Affected by pH and Redox Conditions. In *Biogeodynamics of Pollutants in Soils and Sediments: Risk Assessment of Delayed and Non-Linear Responses*; Salomons, W., Stigliani, W.M., Eds.; Springer: Berlin/Heidelberg, Germany, 1995; pp. 87–102.
124. Schott, J.; Pokrovsky, O.S.; Oelkers, E.H. The Link between Mineral Dissolution/Precipitation Kinetics and Solution Chemistry. *Rev. Mineral. Geochem.* **2009**, *70*, 207–258. [CrossRef]
125. Wiederhold, J. Iron Isotope Fractionation in Soils from Phenomena to Process Identification. Ph.D. Thesis, Eidgenössische Technische Hochschule Zürich, Zürich, Switzerland, 2006.
126. Matthews, A.; Zhu, X.K.; O'Nions, K. Kinetic iron stable isotope fractionation between iron (-II) and (-III) complexes in solution. *Earth Planet. Sci. Lett.* **2001**, *192*, 81–92. [CrossRef]
127. Welch, S.A.; Beard, B.L.; Johnson, C.M.; Braterman, P.S. Kinetic and equilibrium Fe isotope fractionation between aqueous Fe(II) and Fe(III). *Geochim. Cosmochim. Acta.* **2003**, *67*, 4231–4250. [CrossRef]
128. Johnson, C.M.; Skulan, J.L.; Beard, B.L.; Sun, H.; Nealson, K.H.; Braterman, P.S. Isotopic fractionation between Fe(III) and Fe(II) in aqueous solutions. *Earth Planet. Sci. Lett.* **2002**, *195*, 141–153. [CrossRef]
129. Anbar, A.D.; Jarzecki, A.A.; Spiro, T.G. Theoretical investigation of iron isotope fractionation between $Fe(H_2O)_6^{3+}$ and $Fe(H_2O)_6^{2+}$: Implications for iron stable isotope geochemistry. *Geochim. Cosmochim. Acta* **2005**, *69*, 825–837. [CrossRef]
130. Skulan, J.L.; Beard, B.L.; Johnson, C.M. Kinetic and equilibrium Fe isotope fractionation between aqueous Fe(III) and hematite. *Geochim. Cosmochim. Acta* **2002**, *66*, 2995–3015. [CrossRef]

131. Fernandez, A.; Borrok, D.M. Fractionation of Cu, Fe, and Zn Isotopes during the Oxidative Weathering of Sulfide-Rich Rocks. *Chem. Geol.* **2009**, *264*, 1–12. [CrossRef]
132. Rodríguez, N.P.; Engström, E.; Rodushkin, I.; Nason, P.; Alakangas, L.; Öhlander, B. Copper and Iron Isotope Fractionation in Mine Tailings at the Laver and Kristineberg Mines, Northern Sweden. *Appl. Geochem.* **2013**, *32*, 204–215. [CrossRef]
133. Balci, N.; Bullen, T.D.; Witte-Lien, K.; Shanks, W.C.; Motelica, M.; Mandernack, K.W. Iron Isotope Fractionation during Microbially Stimulated Fe(II) Oxidation and Fe(III) Precipitation. *Geochim. Cosmochim. Acta* **2006**, *70*, 622–639. [CrossRef]
134. Brantley, S.L.; Liermann, L.; Bullen, T. Fractionation of Fe Isotopes by Soil Microbes and Organic Acids. *Geology* **2001**, *29*, 535–538. [CrossRef]
135. Beard, B.L.; Johnson, C.M.; Skulan, J.L.; Nealson, K.H.; Cox, L.; Sun, H. Application of Fe Isotopes to Tracing the Geochemical and Biological Cycling of Fe. *Chem. Geol.* **2003**, *195*, 87–117. [CrossRef]
136. Mathur, R.; Ruiz, J.; Titley, S.; Liermann, L.; Buss, H.; Brantley, S. Cu Isotopic Fractionation in the Supergene Environment with and without Bacteria. *Geochim. Cosmochim. Acta* **2005**, *69*, 5233–5246. [CrossRef]
137. Johnson, C.M.; Beard, B.L.; Roden, E.E. The Iron Isotope Fingerprints of Redox and Biogeochemical Cycling in Modern and Ancient Earth. *Annu. Rev. Earth Planet. Sci.* **2008**, *36*, 457–493. [CrossRef]
138. Rodríguez, N.P.; Khoshkhoo, M.; Sandström, Å.; Rodushkin, I.; Alakangas, L.; Öhlander, B. Isotopic Signature of Cu and Fe during Bioleaching and Electrochemical Leaching of a Chalcopyrite Concentrate. *Int. J. Miner. Process.* **2015**, *134*, 58–65. [CrossRef]
139. Falco, L.; Pogliani, C.; Curutchet, G.; Donati, E. A Comparison of Bioleaching of Covellite Using Pure Cultures of *Acidithiobacillus ferrooxidans* and *Acidithiobacillus thiooxidans* or a Mixed Culture of *Leptospirillum ferrooxidans* and *Acidithiobacillus thiooxidans*. *Hydrometallurgy* **2003**, *71*, 31–36. [CrossRef]
140. Garcia, O.; Bigham, J.M.; Tuovinen, O.H. Oxidation of Isochemical FeS_2 (Marcasite-Pyrite) by *Acidithiobacillus Thiooxidans* and *Acidithiobacillus ferrooxidans*. *Miner. Eng.* **2007**, *20*, 98–101. [CrossRef]
141. Tributsch, H. Direct versus indirect bioleaching. *Hydrometallurgy* **2001**, *59*, 177–185. [CrossRef]
142. Natarajan, K.A. Microbial Aspects of Acid Mine Drainage and Its Bioremediation. *Trans. Nonferrous Met. Soc. China (Engl. Ed.)* **2008**, *18*, 1352–1360. [CrossRef]
143. Brantley, S.L.; Liermann, L.J.; Guynn, R.L.; Anbar, A.; Icopini, G.A.; Barling, J. Fe Isotopic Fractionation during Mineral Dissolution with and without Bacteria. *Geochim. Cosmochim. Acta* **2004**, *68*, 3189–3204. [CrossRef]
144. Wasylenki, L.E.; Anbar, A.D.; Liermann, L.J.; Mathur, R.; Gordon, G.W.; Brantley, S.L. Isotope Fractionation during Microbial Metal Uptake Measured by MC-ICP-MS. *J. Anal. At. Spectrom.* **2007**, *22*, 905. [CrossRef]
145. Croal, L.R.; Johnson, C.M.; Beard, B.L.; Newman, D.K. Iron isotope fractionation by Fe(II)-oxidizing photoautotrophic bacteria [1]. *Geochim. Cosmochim. Acta* **2004**, *68*, 1227–1242. [CrossRef]
146. Hubbard, C.G.; Black, S.; Coleman, M.L. Aqueous Geochemistry and Oxygen Isotope Compositions of Acid Mine Drainage from the Río Tinto, SW Spain, Highlight Inconsistencies in Current Models. *Chem. Geol.* **2009**, *265*, 321–334. [CrossRef]
147. Malmström, M.E.; Destouni, G.; Banwart, S.A.; Strömberg, B.H.E. Resolving the Scale-Dependence of Mineral Weathering Rates. *Environ. Sci. Technol.* **2000**, *34*, 1375–1378. [CrossRef]
148. Liu, R.; Wolfe, A.L.; Dzombak, D.A.; Stewart, B.W.; Capo, R.C. Comparison of Dissolution under Oxic Acid Drainage Conditions for Eight Sedimentary and Hydrothermal Pyrite Samples. *Environ. Geol.* **2008**, *56*, 171–182. [CrossRef]
149. Matthies, R.; Aplin, A.C.; Boyce, A.J.; Jarvis, A.P. Geochemical and Stable Isotopic Constraints on the Generation and Passive Treatment of Acidic, Fe–SO_4 Rich Waters. *Sci. Total Environ.* **2012**, *420*, 238–249. [CrossRef]